# CHAPTER IV
# RESULTS AND DISCUSSION

## 4.1 Characterization of Benzoxazine Monomers

### 4.1.1 Structural Characterization of 3,4-Dihydro-6-methoxy-3-propyl-2H-1,3-benzoxazine, 1

FTIR (KBr, $cm^{-1}$): 1498 (vs, oxazine), 1218 (vs, C-O-C asymmetric stretching), 1041 (s, C-O-C symmetric stretching). MS: m/z (relative intensity, %) 70 (3), 71 (5), 136 (20), 137 (20), 149 (6), 192 (2), 194 (1), 206 (100), 207 (61), 208 (33), 209 (5), 220 (4), 345 (11), 414 (1), 415 (6), 416 (2).

The peak at 206 referred the molecular weight of monomer **1** (Figure 4.2). The peak observed at 137 implied the breakage of C-N bond in oxazine ring to give fragment **a** as proposed in Scheme 4.1. The fragment **b** gives the peak at 71. The assembly of two monomeric units gives the peak at 415. However, the peak intensity implied that single molecule of monomer is a preferable structure.

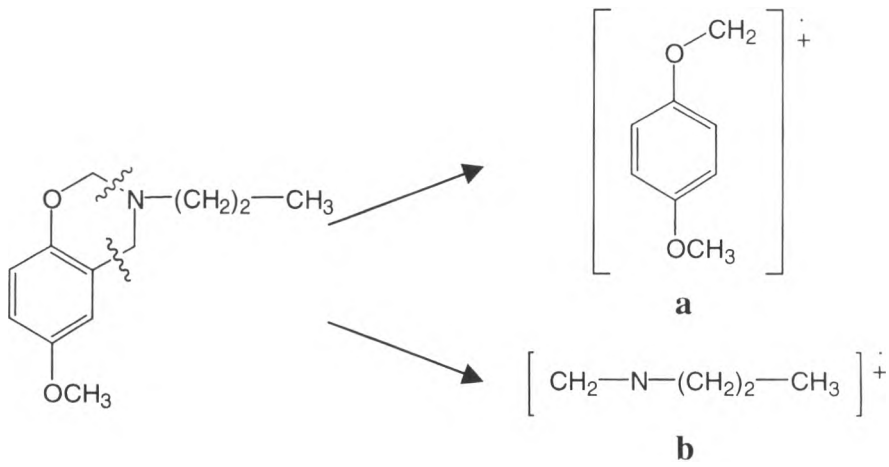


**Scheme 4.1** Possible fragmentation of **1**, (a) m/z = 136, (b) m/z = 71.

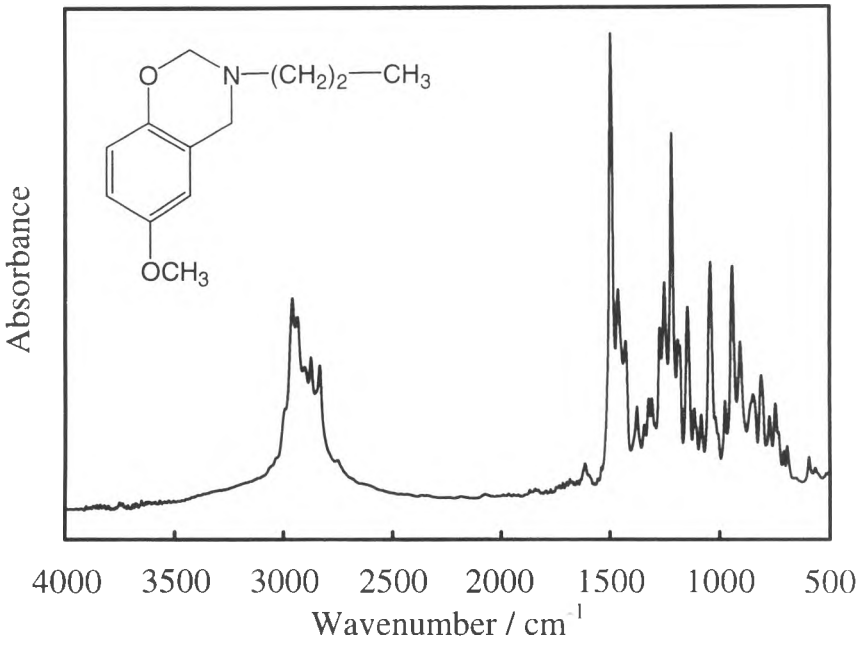


**Figure 4.1** FTIR spectrum of **1**.

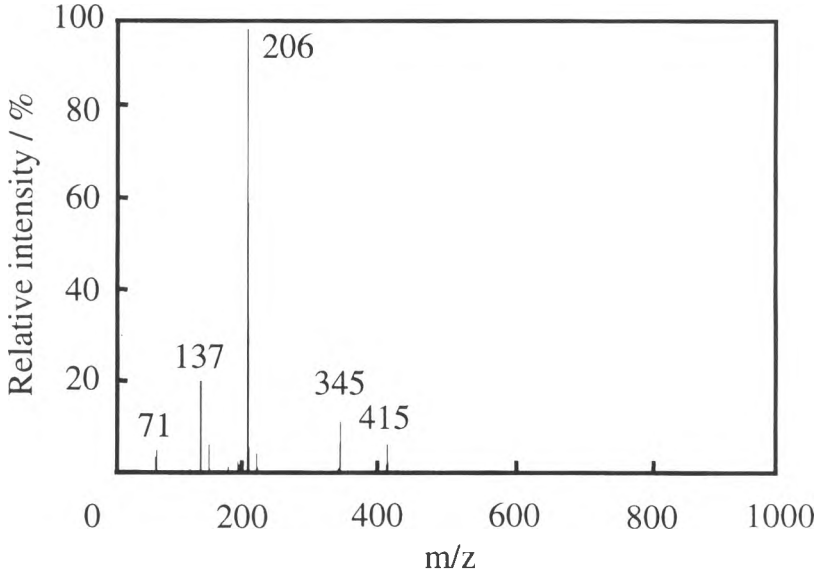


**Figure 4.2** MS spectrum of **1**.

4.1.2 Structural Characterization of 3,4-Dihydro-6-methyl-3-propyl-2H-1,3-benzoxazine, **2**

FTIR (KBr, $cm^{-1}$): 1502 (vs, oxazine), 1223 (vs, C-O-C asymmetric stretching), 1120 (s, C-O-C symmetric stretching).

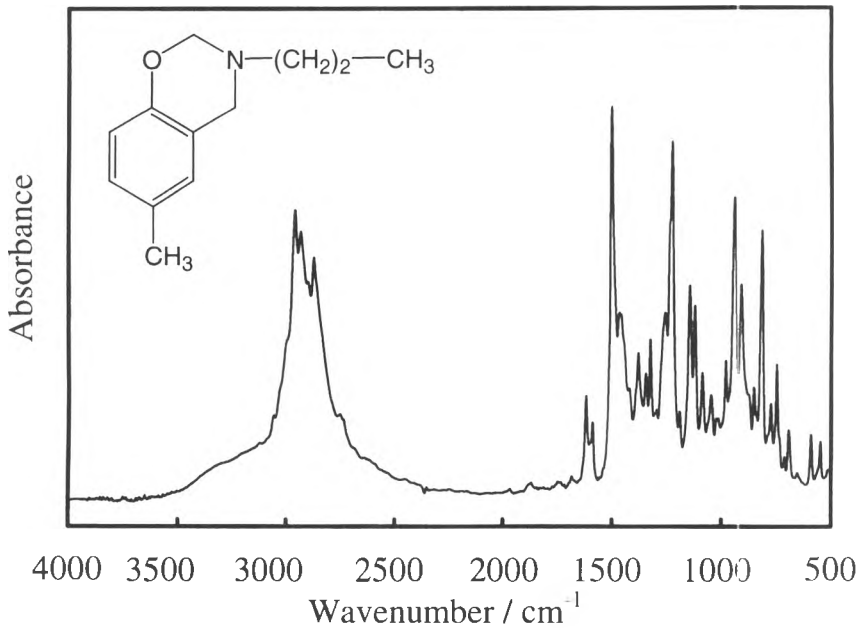


**Figure 4.3** FTIR spectrum of **2**.

## 4.2 Characterization of Benzoxazine Dimers

The crude products **3,** and **4** were yellowish powder. The products were recrystallized to obtain a colorless clear crystal. Each product was characterized as follows.

4.2.1 Structural Characterization of N,N-bis (5-methoxy-2-hydroxy benzyl) propylamine, **3**

FTIR (KBr, $cm^{-1}$): 3281 (s, O-H stretching), 1497 (vs, C-N stretching), 1243 (vs, C-O asymmetric stretching), 1044 (vs, C-O symmetric stretching). $^1$H-NMR (in $CDCl_3$, δ values in ppm from TMS): δ 0.85 (3H, t,

N-$CH_2$-$CH_2$-**$CH_3$**), 1.63 (2H, m, N-$CH_2$-**$CH_2$**-$CH_3$), 2.50 (2H, t, N-**$CH_2$**-$CH_2$-$CH_3$), 3.68 (4H, s, Ar-**$CH_2$**-N), 3.71 (6H, s, AR-O-**$CH_3$**), 6.63-6.73 (6H, Ar-**H**). Anal Calcd. for $C_{19}H_{25}O_4N$: (%) C, 68.86; H, 7.60; O, 19.31; N, 4.23. Found: (%) C, 68.70; H, 7.34; O, 17.99; N, 5.97. MS: m/z (relative intensity, %) 136 (2), 137 (82), 185 (3), 194 (4), 195 (1), 196 (5), 331 (12), 332 (100), 333 (8). Yield (%): 8.67. TLC (EtOAc: $CHCl_3$; 3: 2, $R_f$): 0.72.

Figure 4.6 shows mass spectrum of **3**. The peak at 332 represents molecular weight of **3**. The peak at 137 is as high as the main peak at 332. This implied the breaking of C-N bond as shown in Scheme 4.2. The presence of fragment **a** is well supported by the intramolecular hydrogen bonding formed in the structure. It should be noted that, different from **1**, the two cluster aggregation of **3** was not observed.

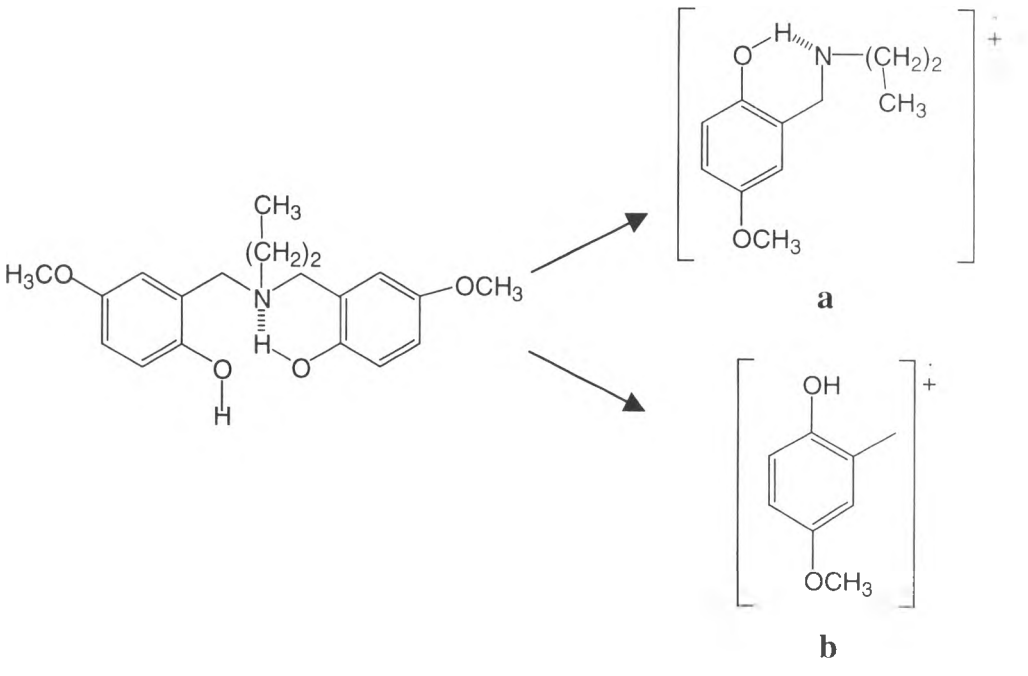


**Scheme 4.2** Possible fragmentation of **3,** (a) m/z = 194, (b) m/z = 137.

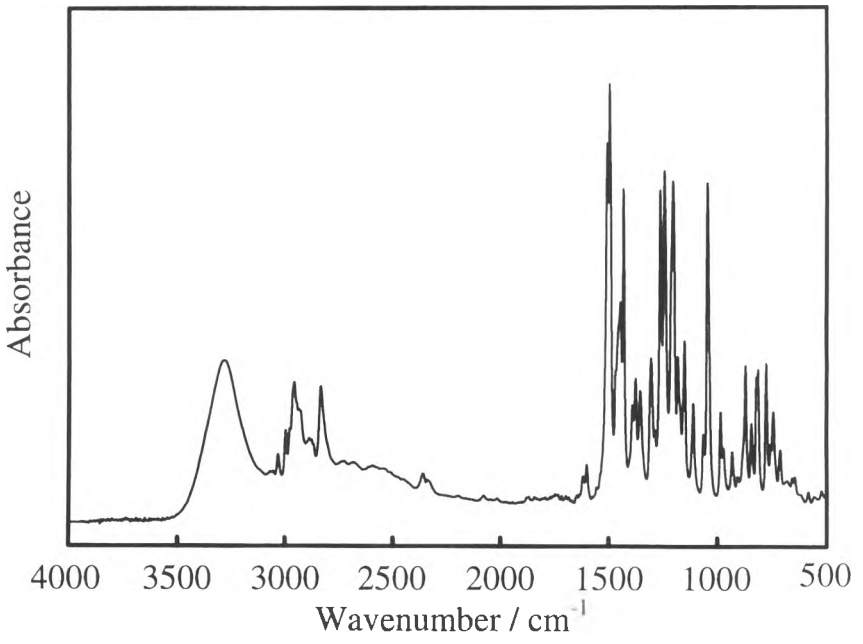


**Figure 4.4** FTIR spectrum of **3**.

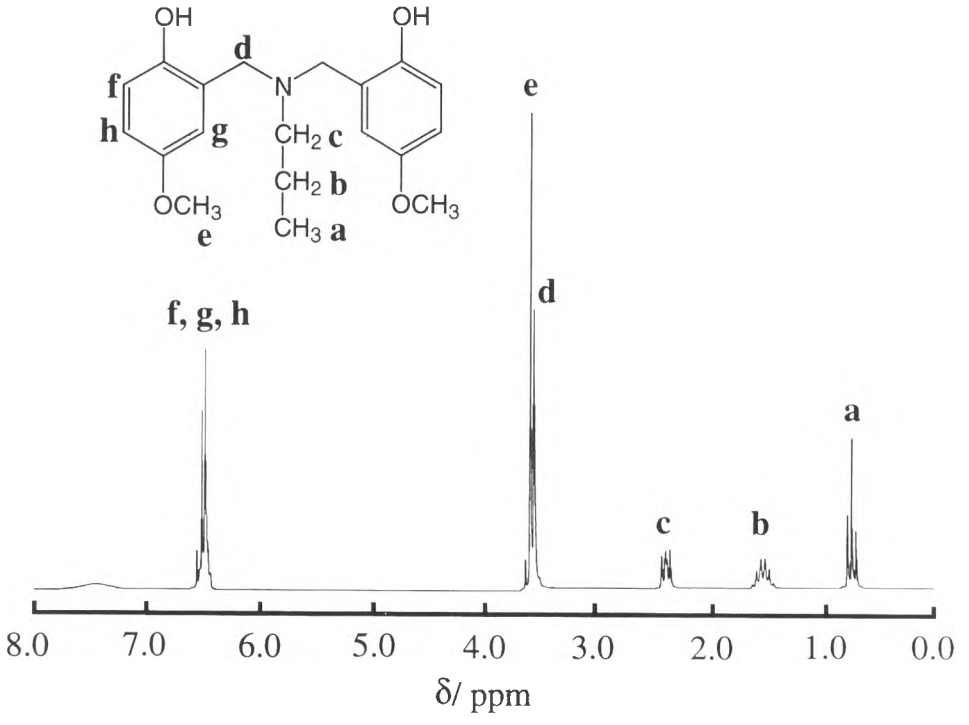


**Figure 4.5** $^{1}$H-NMR spectrum of **3**.

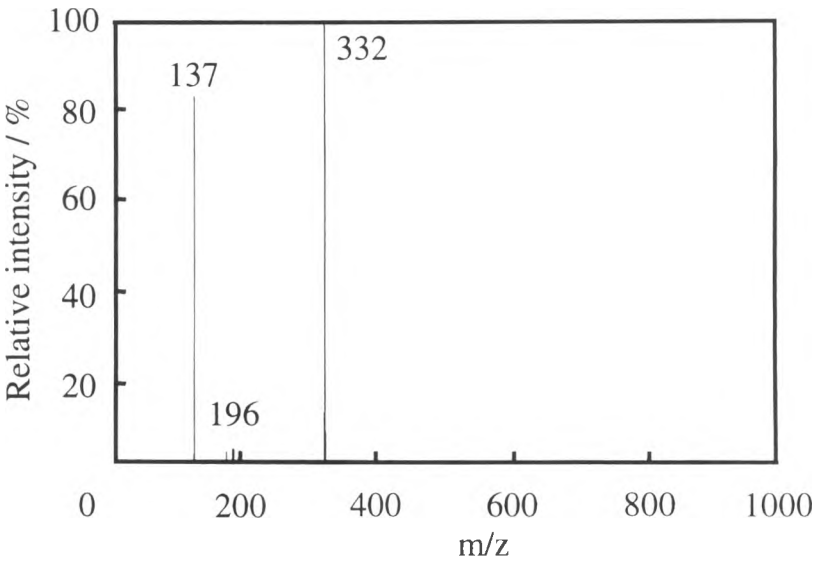


**Figure 4.6** MS spectrum of **3**.

4.2.2 Structural Characterization of N,N-bis (5-methyl-2-hydroxy benzyl) propylamine, **4**

FTIR (KBr, $cm^{-1}$): 3250 (s, O-H stretching), 1501 (vs, C-N stretching). $^1$H-NMR (in $CDCl_3$, δ values in ppm from TMS): δ 0.87 (3H, t, N-$CH_2$-$CH_2$-**$CH_3$**), 1.65 (2H, m, N-$CH_2$-**$CH_2$**-$CH_3$), 2.20 (6H, s, AR-**$CH_3$**), 2.51 (2H, t, N-**$CH_2$**-$CH_2$-$CH_3$), 3.68 (4H, s, Ar-**$CH_2$**-N), 6.68 (2H, d, Ar-**H**), 6.84 (2H, s, Ar-**H**), 6.91 (2H, d, Ar-**H**). TLC (EtOAc: $CHCl_3$; 3: 2, $R_f$): 0.81.

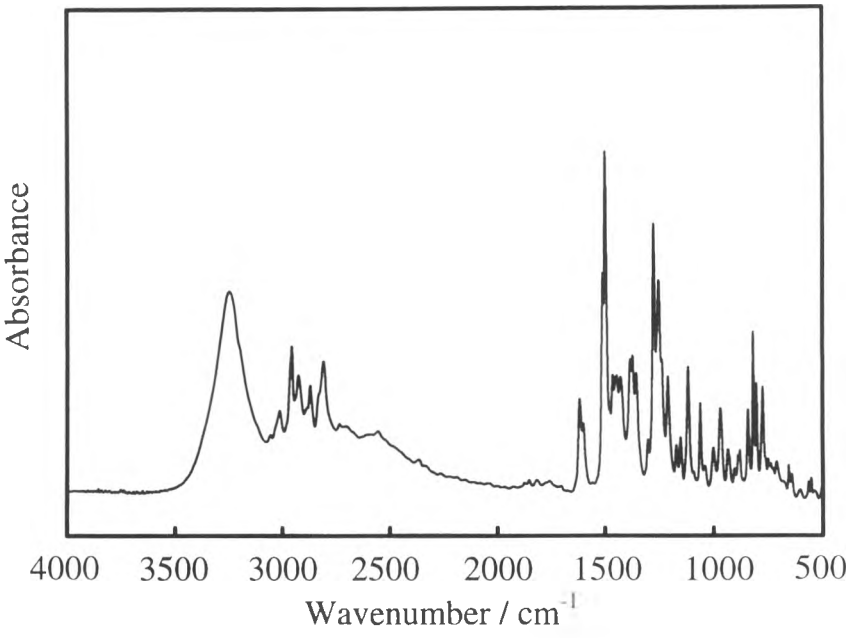


**Figure 4.7** FTIR spectrum of **4**.

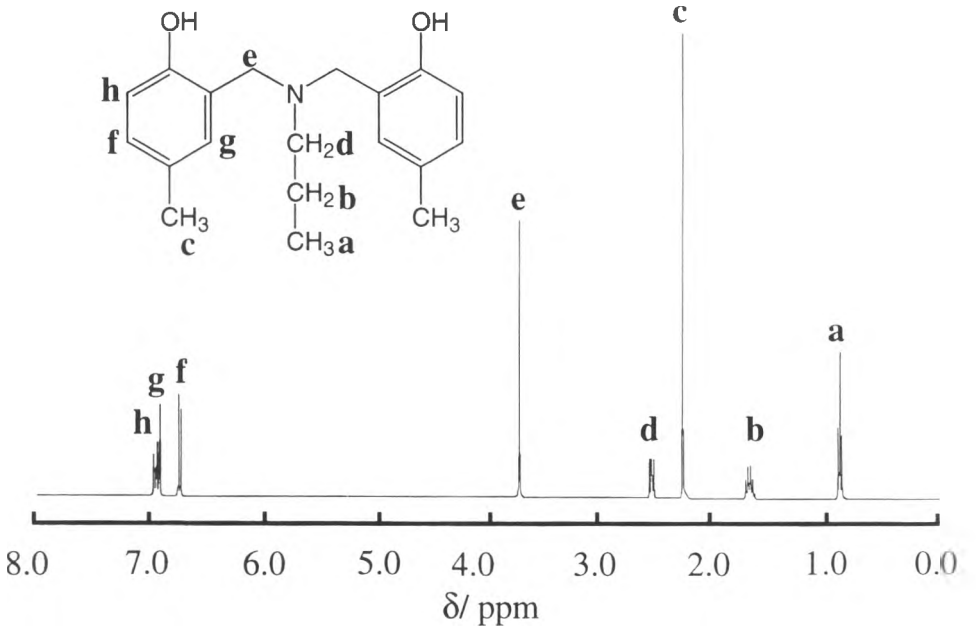


**Figure 4.8** $^{1}$H-NMR spectrum of **4**.

## 4.3 Characterization of Esterified Dimers

### 4.3.1 Structural Characterization of N,N-bis (5-methoxy-2-benzoyl benzyl) propylamine, **5**

FTIR (KBr, $cm^{-1}$): 1737 (vs, C=O stretching), 1497 (vs, C-N stretching). $^1$H-NMR (in $CDCl_3$, δ values in ppm from TMS): δ 0.76 (3H, t, N-$CH_2$-$CH_2$-**$CH_3$**), 1.43 (2H, m, N-$CH_2$-**$CH_2$**-$CH_3$), 2.34 (2H, t, N-**$CH_2$**-$CH_2$-$CH_3$), 3.49 (4H, s, Ar-**$CH_2$**-N), 3.79 (6H, s, AR-O-**$CH_3$**), 6.81 (2H, d, Ar-**H**), 6.97 (2H, s, Ar-**H**), 7.20 (2H, d, Ar-**H**), 7.42 (4H, t, Ar-**H**), 7.61 (2H, t, Ar-**H**), 8.15 (4H, d, Ar-**H**). TLC (MeOH: $CHCl_3$; 1: 19, $R_f$): 0.24.

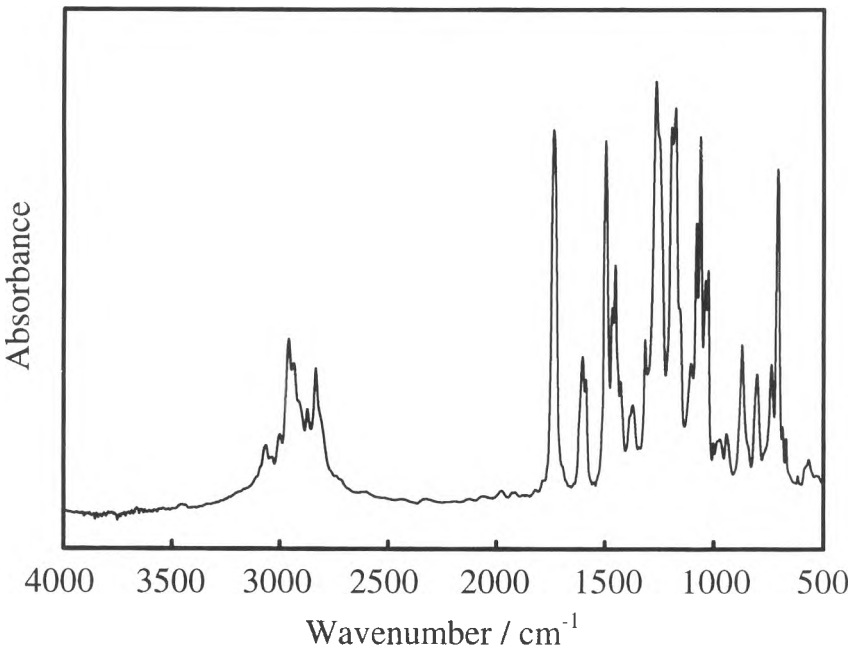


**Figure 4.9** FTIR spectrum of **5**.

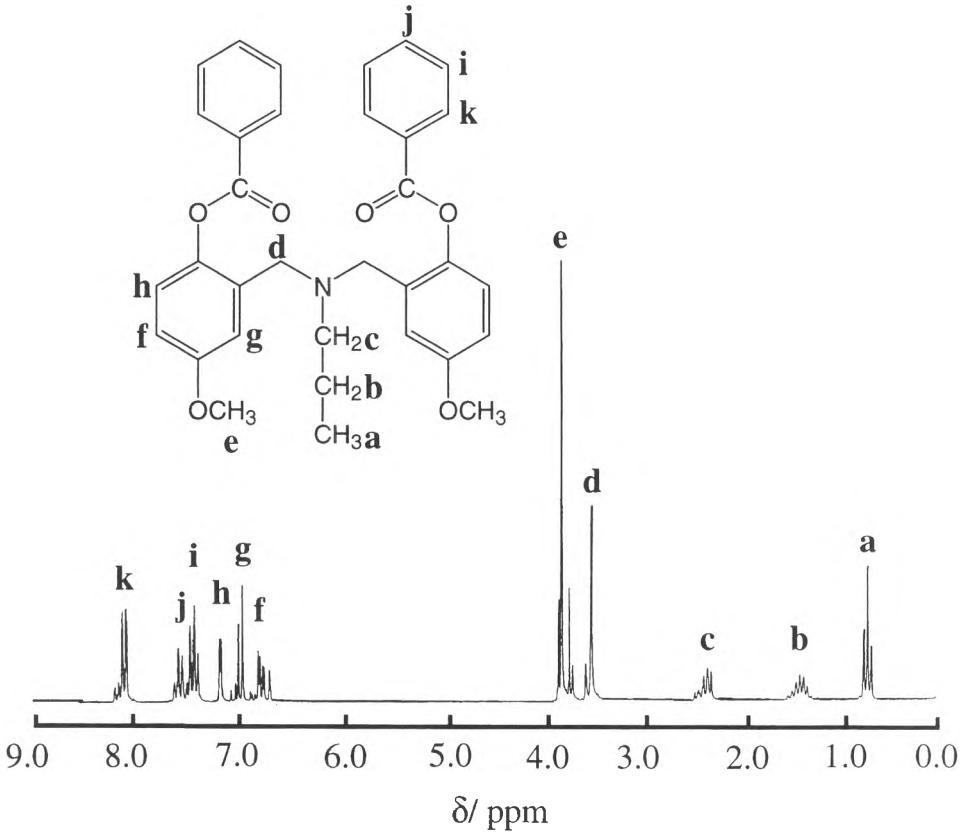


**Figure 4.10** $^{1}$H-NMR spectrum of **5**.

4.3.2 Structural Characterization of N,N-bis (5-methyl-2-benzoyl benzyl) propylamine, **6**

FTIR (KBr, $cm^{-1}$): 1737 (vs, C=O stretching), 1497 (s, C-N stretching). $^{1}$H-NMR (in $CDCl_3$, δ values in ppm from TMS): δ 0.72 (3H, t, N-$CH_2$-$CH_2$-**$CH_3$**), 1.38 (2H, m, N-$CH_2$-**$CH_2$**-$CH_3$), 1.57 (6H, s, Ar-**$CH_3$**), 2.34 (2H, t, N-**$CH_2$**-$CH_2$-$CH_3$), 3.48 (4H, s, Ar-**$CH_2$**-N), 6.92 (2H, d, Ar-**H**), 7.06 (2H, d, Ar-**H**), 7.36 (2H, s, Ar-**H**), 7.47 (4H, t, Ar-**H**), 7.62 (2H, t, Ar-**H**), 8.16 (4H, d, Ar-**H**). TLC (MeOH: $CHCl_3$; 1: 19, $R_f$): 0.38.

It should be noted that proton at position **c** was shifted to 1.57 ppm as compared to position **c** at 2.20 of compound **4**. This might be due to the electron conjugation structure along four phenyl rings which induced the electron rich through all structure.

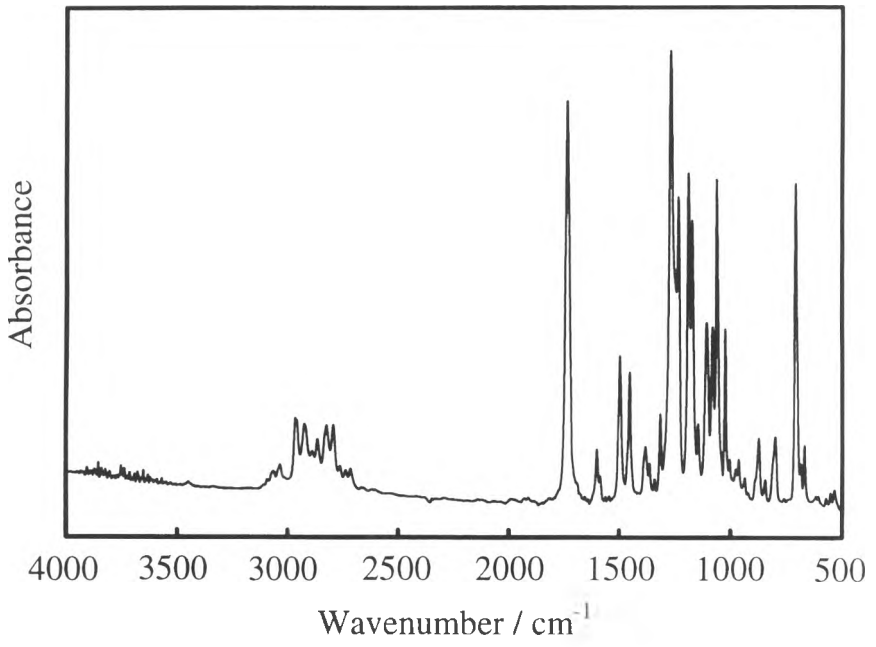


**Figure 4.11** FTIR spectrum of **6**.

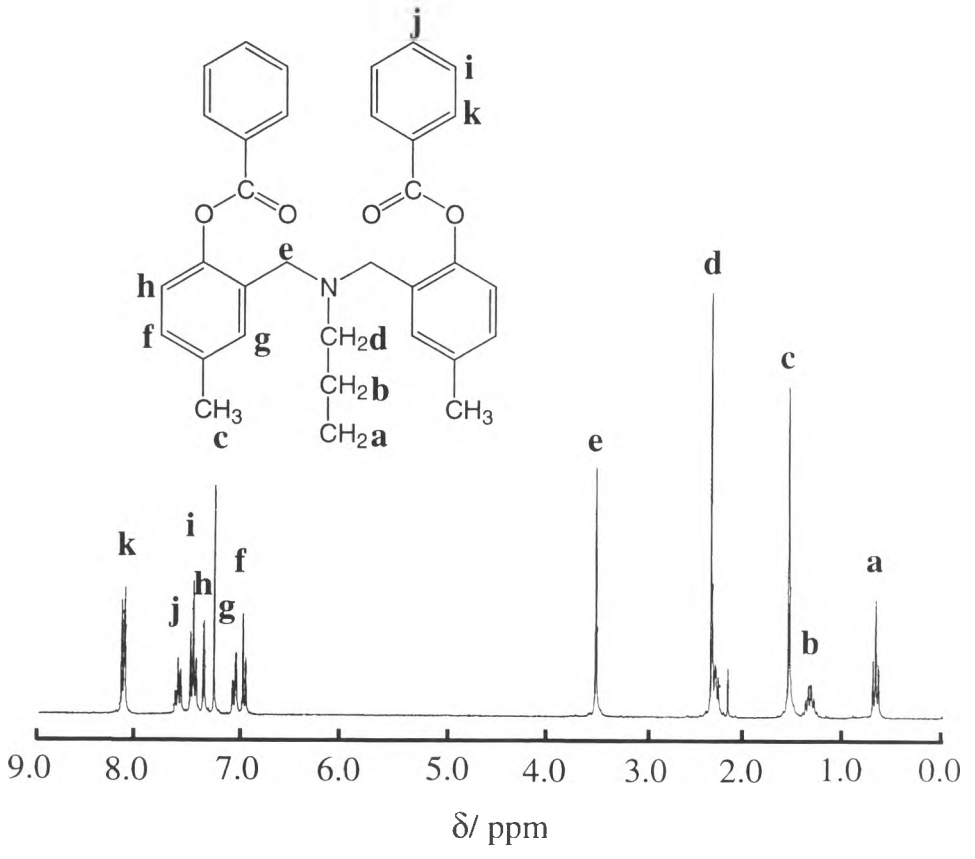


**Figure 4.12** $^{1}$H-NMR spectrum of **6**.

## 4.4 Structural Characterization of Cyclic Oligomer, 7

FTIR (KBr, $cm^{-1}$): 1735 (vs, C=O stretching), 1493 (s, C-N stretching), 1266 (vs, C-O asymmetric stretching, ester), 1248 (vs, C-O asymmetric stretching, ether), 1178 (vs, C-O symmetric stretching, ester), 1075 (s, C-O symmetric stretching, ether). $^1$H-NMR (in $CDCl_3$, δ values in ppm from TMS): δ 0.89 (6H, t, N-$CH_2$-$CH_2$-**$CH_3$**), 1.50 (4H, m, N-$CH_2$-**$CH_2$**-$CH_3$), 2.30 (4H, t, N-**$CH_2$**-$CH_2$-$CH_3$), 3.37 (8H, s, Ar-**$CH_2$**-N), 3.84 (12H, s, Ar-O-**$CH_3$**), 6.82 (4H, d, Ar-**H**), 7.02 (4H, d, Ar-**H**), 7.32 (4H, s, Ar-**H**), 8.26 (8H, s, Ar-**H**). Anal Calcd. for $C_{54}H_{54}O_{12}N_2$: (%)C, 70.27; H, 5.90; O, 20.80; N, 3.04. Found: (%) C, 70.07; H, 5.76; O, 20.12; N, 4.05. Yield (%): 23.37. TLC (MeOH: $CHCl_3$; 1: 19, $R_f$): 0.69.

The possible cyclic structure of **7** can either be a dimer or a tetramer ring. Although FTIR, $^1$H-NMR, and EA implied the successful cyclization, the composition of ring unit could not be clarified. MS in TOF (Time of Flight) mode is a useful technique which can determine the molecular weight of the main species in compound. $^1$H-NMR spectrum shows a singlet peak of proton **i** belonging to benzene ring in ester linkage. This is due to the symmetry of all protons of this phenyl ring.

The calculated molecular weight of cyclic compound for dimer and tetramer type are 462, and 923 g/mol, respectively. Figure 4.15 shows m/z at 917 which is close to that of the tetramer type. The peak at 400, although, might be claimed as a dimer type, the value was too low to conclude as a dimer peak. Thus, at present, we concluded that the compound obtained is a tetramer cyclic.

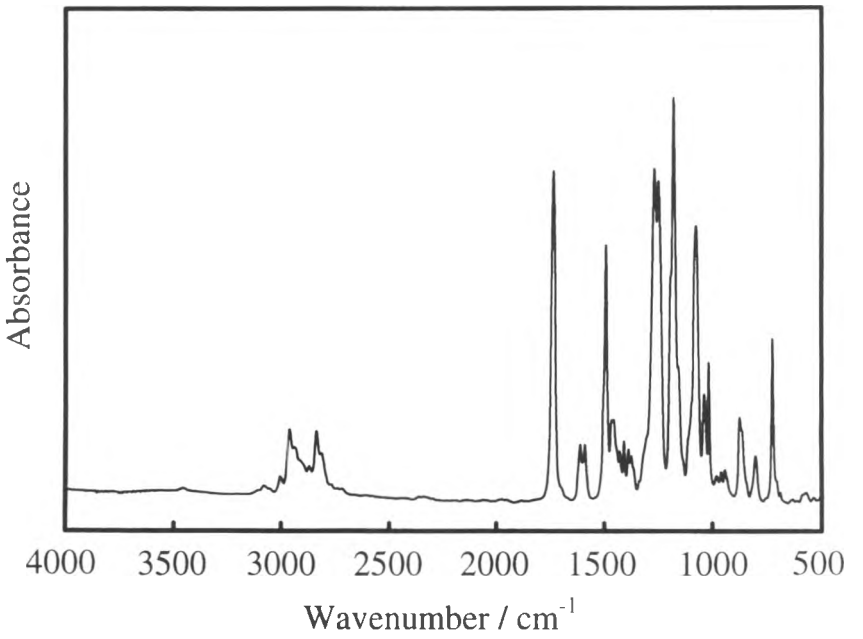


**Figure 4.13** FTIR spectrum of **7**.

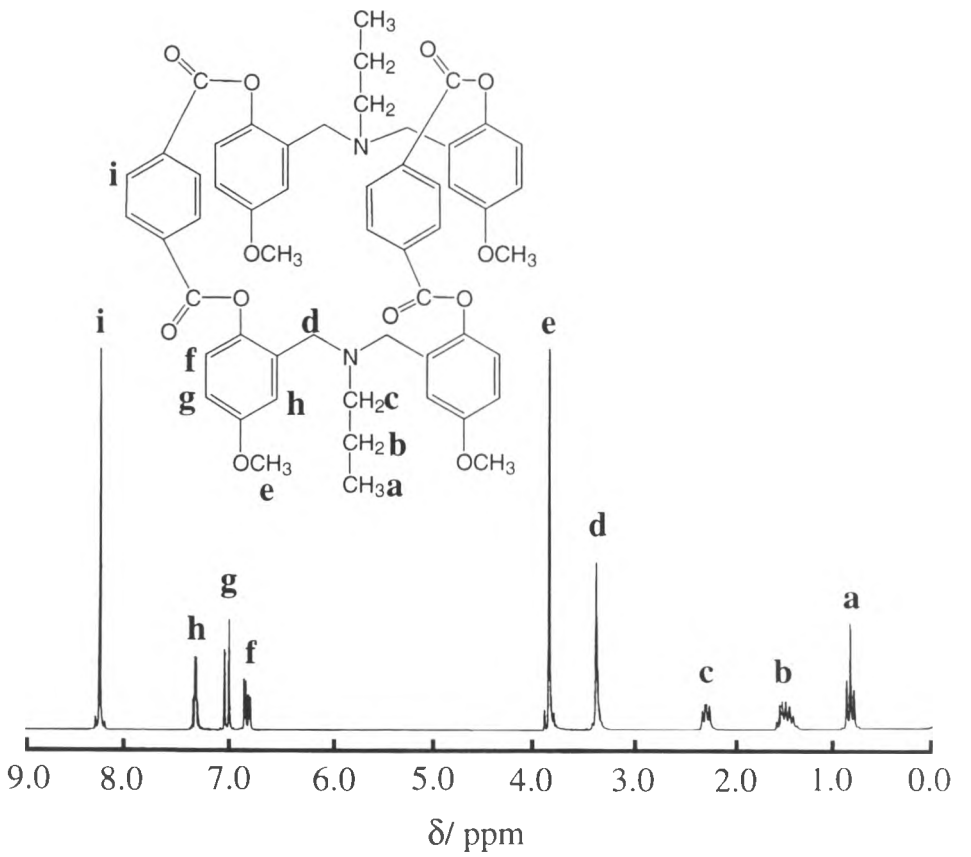


**Figure 4.14** $^{1}$H-NMR spectrum of **7**.

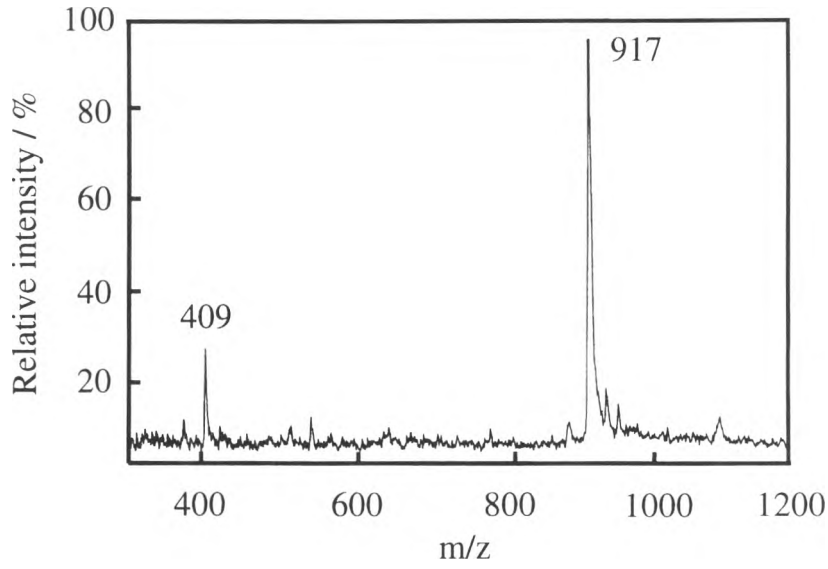


**Figure 4.15** MS spectrum of **7**.

## 4.5 Ion Extraction Studies

Ion extraction studies were done via Pedersen's technique which is semiquantitative means of assessing ion transfer ability from aqueous phase to organic phase.

Dimers **3**, and **4** show high sensitivity but low selectivity on sodium and potassium picrates as shown in Figures 4.16, and 4.17. As concentration of dimer increases, the ion extraction increases. Although **3** was expected to perform much higher ion extraction ability than that of **4**, the result was turned out to be another way. As shown in Figure 4.18, ion extraction percentage of **4** is slightly higher than that of **3**. Chirachanchai *et al.* (in preparation) reported the existence of strong inter- and intramolecular hydrogen bonding in the structure of N,N-bis (5-methyl-2-hydroxybenzyl) cyclohexylamine, N,N-bis (5-ethyl-2-hydroxybenzyl) cyclohexylamine, and N,N-Bis (5-methyl-2-hydroxybenzyl) propylamine by using X-ray crystallography. Taking this into the consideration, the ion extraction ability of **3** might be affected by the

strong hydrogen bonding network. Here, we proposed that in the case of **4**, the hydrogen bonding was formed at only 2 positions while that of **3** might be formed at 3 positions, as indicated in Scheme 4.3. As a result, additional electrons from methoxy group did not play anyrole in ion extraction ability.

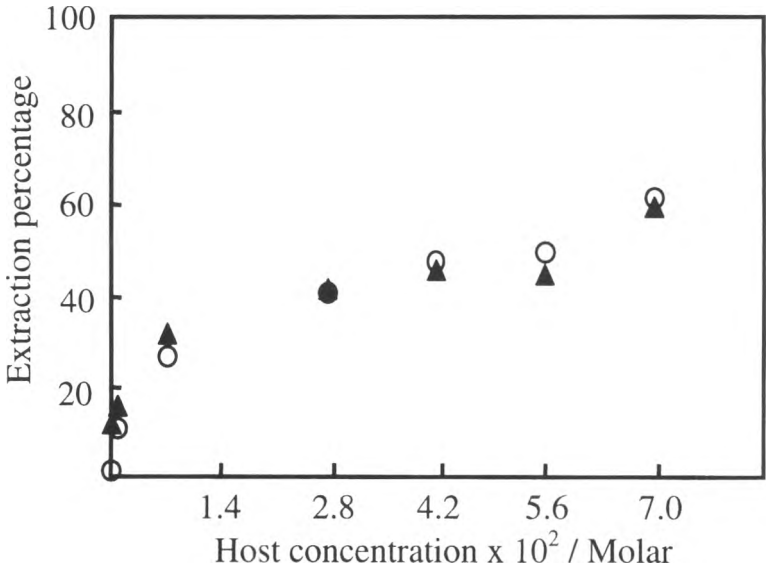


**Figure 4.16** Ion extraction of **3** with ○) Na; ▲) K, at picrate salt concentration $7x10^{-5}$ M.

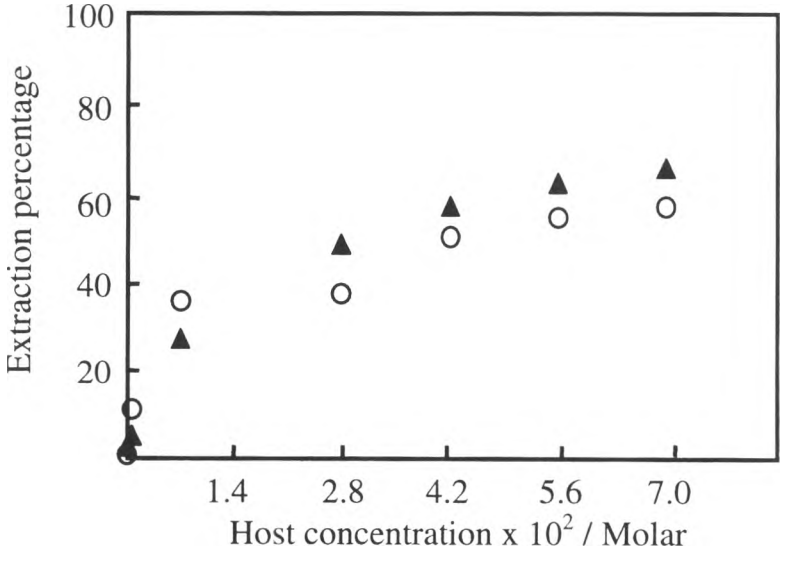


**Figure 4.17** Ion extraction of **4** with ○) Na; ▲) K, at picrate salt concentration $7x10^{-5}$ M.

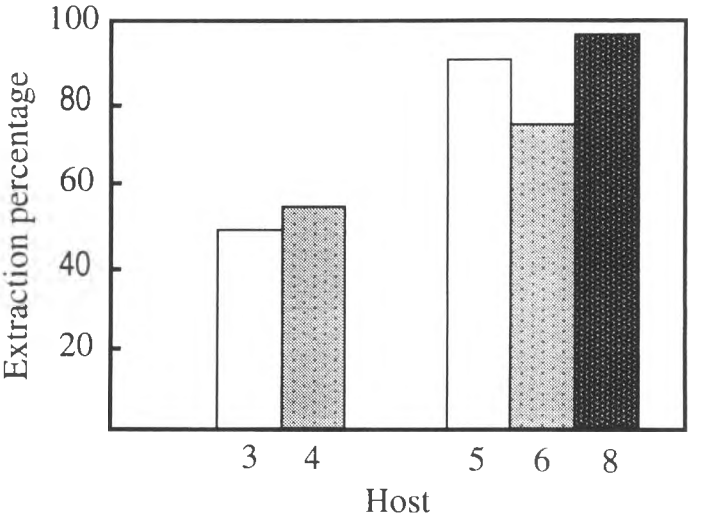


**Figure 4.18** Extraction percentage of benzoxazine dimer derivatives **3-6**, and **8** at concentration $5.6 \times 10^{-2}$ M with sodium picrate at concentration $7 \times 10^{-5}$ M.

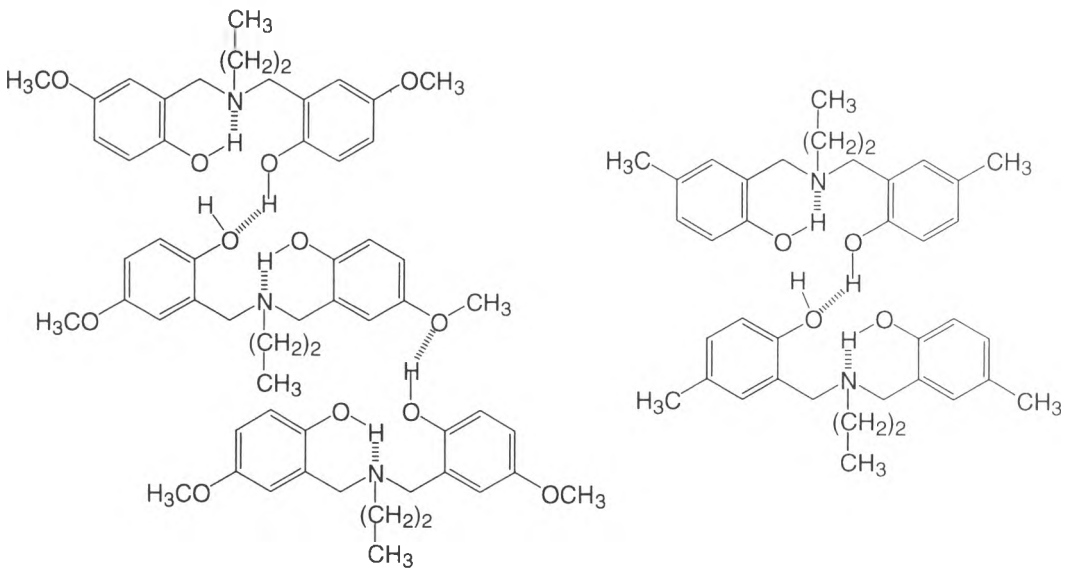

**3** **4**

**Scheme 4.3** Expected hydrogen bonding network in **3**, and **4**.

For esterified dimer, the ion extraction ability reaches its maximum at above concentration $7\times10^{-3}$ M for **5**, and **6** (Figures 4.19, and 4.20).

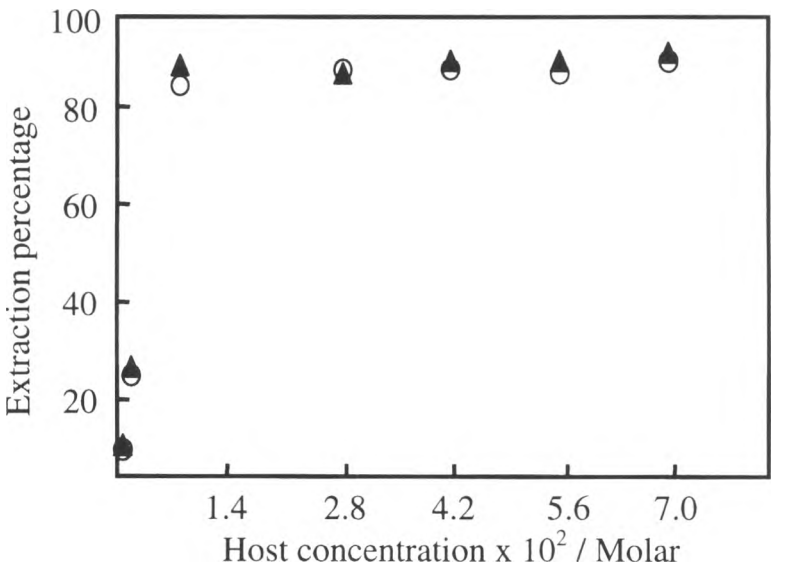


**Figure 4.19** Ion extraction of **5** with ○) Na; ▲) K, at picrate salt concentration $7x10^{-5}$ M.

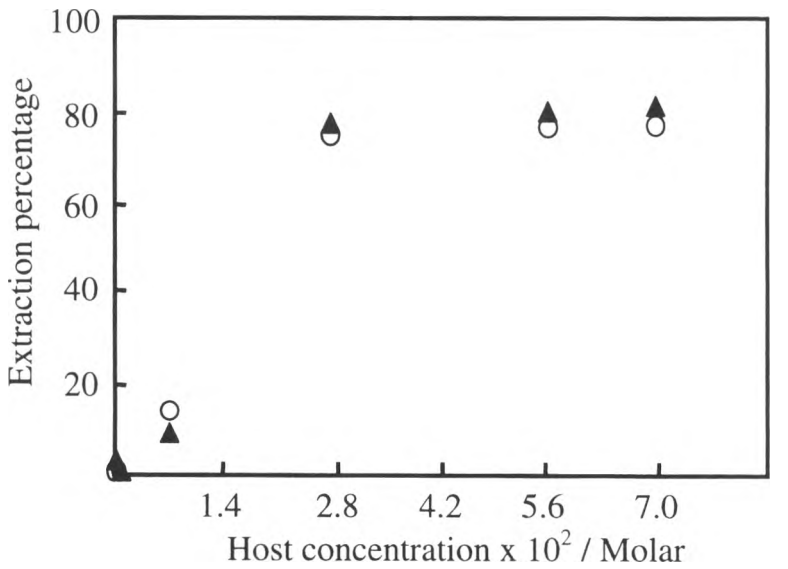


**Figure 4.20** Ion extraction of **6** with ○) Na; ▲) K, at picrate salt concentration $7x10^{-5}$ M.

This implied that the complexation with metal ion would be formed effectively at above the concentration of $7\times10^{-3}$ M. It should be noted that extraction properties become more significant than that of benzoxazine dimer. Techakamolsuk *et al.* reported that when the hydrogen bonding was eliminated and more lone pair electrons were provided from ester groups to the system, the ion extraction ability would be enhanced. Here, it was found that **5** exhibited metal ion interaction more significant than that of **6** (Figure 4.18). This might be due to the high electron density in structure from both ester and methoxy groups of phenol unit, as proposed in Scheme 4.4.

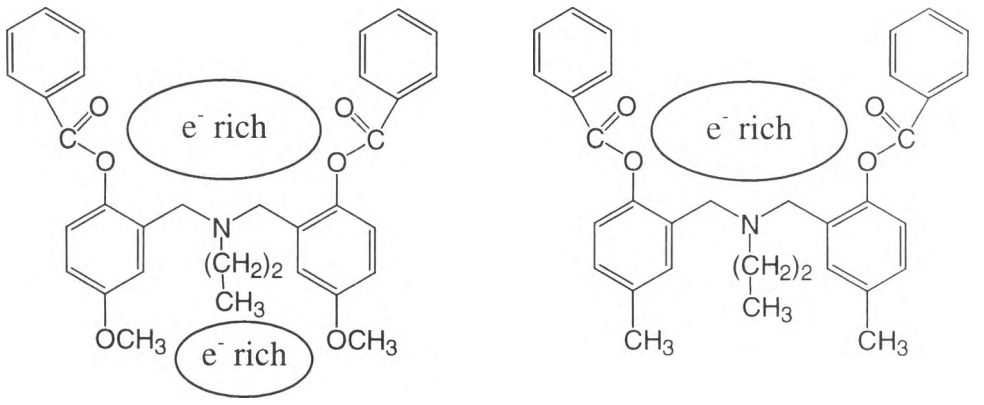


**5** **6**

**Scheme 4.4** Expected structures with high electron density region of **5**, and **6**.

Comparing **6** to **8** (Techakamolsuk *et al.*,1999) (Scheme 4.5), **6** showed slightly lower extraction percentage than that of **8** (Figure 4.18). This implied that the more bulky group on N atom, the lower extraction ability. Techakamolsuk *et al.* concluded that when esterified benzoxazine dimer consisted of less bulky group on N atom, the ion extraction ability was significant. Taking **5** and **8** in consideration (Scheme 4.5), even though **8** has less bulky group attached to N atom, but both compounds gave nearly similar

extraction percentage (Figure 4.18). This implied that ion extraction ability of esterified benzoxazine dimer was enhanced by two factors, i.e., the packing structure with more cavity and functional group with more electron density.

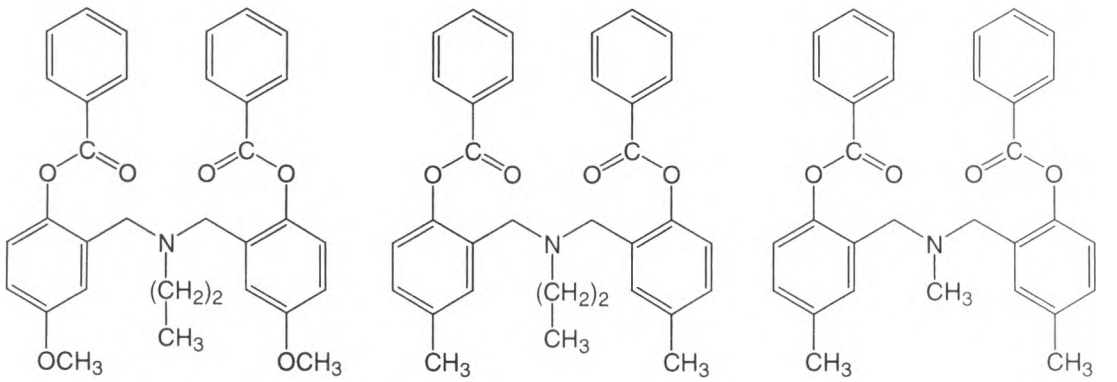

**5** **6** **8**

**Scheme 4.5** Structures of **5**, **6**, and **8** (Techakamolsuk *et al.*, 1999).

In the case of cyclic oligobenzoxazine, **7**, metal ion extraction could not be observed even the host concentration was increased for 100 times higher than that of metal picrate (Figure 4.21). This implied that the cavity size was not suitable with sodium and potassium ions. It is important to clarify in the future that compound 7 may show inclusion property with large metal ion size or even neutral molecules.

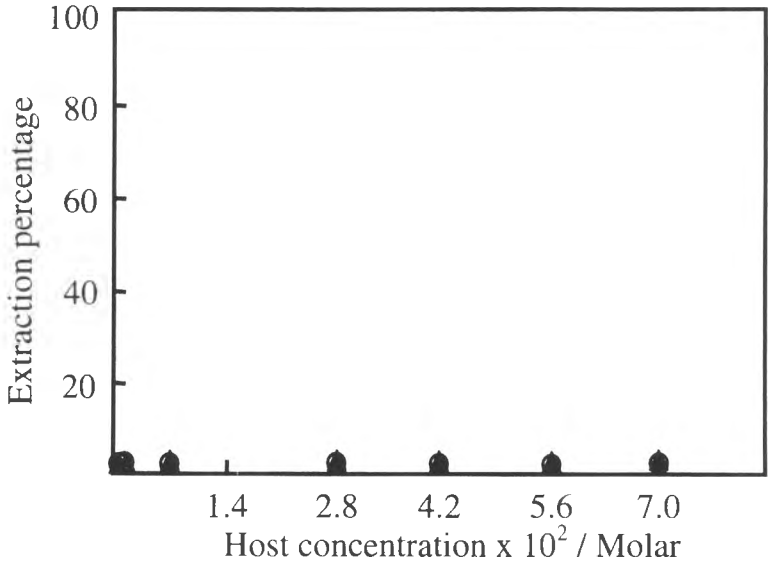


**Figure 4.21** Ion extraction of **7** with ○) Na; ▲) K, at picrate salt concentration $7x10^{-5}$ M.